



## POSSIBLE CARDIOPROTECTIVE MECHANISM OF ACTION OF DEXRAZOXANE, AND PROBABLE HUMAN TOPOISOMERASE II $\beta$ INHIBITORS: AN *IN SILICO* ANALYSIS

*DEKSRAZOKSANIN OLASI KARDİYOPROTEKTİF ETKİ MEKANİZMASI VE MUHTEMEL  
İNSAN TOPOİZOMERAZ IIB İNHİBİTÖRLERİ: İN SİLİCO ANALİZ*

Fuat KARAKUŞ<sup>1\*</sup> , Burak KUZU<sup>2</sup> 

<sup>1</sup>Van Yüzüncü Yıl University, Faculty of Pharmacy, Department of Pharmaceutical Toxicology,  
65080, Van, Turkey

<sup>2</sup>Van Yüzüncü Yıl University, Faculty of Pharmacy, Department of Pharmaceutical Chemistry, 65080,  
Van, Turkey

### ABSTRACT

**Objective:** *The aim of this study was to determine which metabolite plays a role in the cardioprotective effect of dexrazoxane, and also to identify alternative compounds to dexrazoxane since clinical use of dexrazoxane is limited. For this purpose, the interactions of dexrazoxane and its three metabolites (B, C, and ADR-925), as well as the compounds, which reported to be inhibitors for topoisomerase VI (prototype of human DNA topoisomerase II beta), with human DNA topoisomerase II beta were investigated by molecular docking. Afterwards, the theoretical ADMET properties of all these compounds were determined*

**Material and Method:** *The molecular structures were optimized by Gaussview 05 and Gaussian 03 package programs. AutoDock 4.2 software was used for molecular docking studies and the docking complexes were analyzed in 2D and 3D using the Discovery Studio Client 4.1 program. The pkCSM online program was used to calculate the theoretical ADMET parameters.*

**Result and Discussion:** *As a result of molecular docking studies, it was determined that the B metabolite of dexrazoxane has a higher binding potential to human DNA topoisomerase II beta compared to both dexrazoxane and its other metabolites. The binding potentials of other compounds reported in the literature to human DNA topoisomerase II beta were radicicol>quinacrine>purpurin>9-Aminoacridine>hexylresorcinol, respectively.*

\* **Corresponding Author / Sorumlu Yazar:** Fuat Karakuş  
**e-mail / e-posta:** fuatkarakus@yyu.edu.tr, **Phone / Tel.:** +90 432 444 5065 (21185)

*The results showed that the B metabolite of dexrazoxane plays an important role in the cardioprotective mechanism of action of dexrazoxane against anthracycline cardiotoxicity. In addition, it has been determined that other compounds, except purpurin, have the potential to cause toxicity.*

**Keywords:** Anthracycline cardiotoxicity, cardioprotective agents, dexrazoxane, *in silico* analysis, topoisomerase II inhibitors

## ÖZ

**Amaç:** Bu çalışmanın amacı deksrazoksanın kardioprotektif etkisinde hangi metabolitinin rol oynadığını belirlemek ve ayrıca deksrazoksanın klinik kullanımı sınırlı olduğu için deksrazoksana alternatif bileşikler saptamaktır. Bu amaçla, deksrazoksana ve üç metabolitinin (B, C, ve ADR-925) ve ayrıca literatürde topoizomerez VI (insan DNA topoizomerez II beta'nın prototipi) için inhibitör olduğu bildirilen bileşiklerin insan DNA topoizomerez II beta ile etkileşimleri moleküler kenetleme ile araştırıldı. Sonrasında tüm bu bileşiklerin teorik ADMET özellikleri belirlendi.

**Gereç ve Yöntem:** Moleküler yapılar Gaussview 05 ve Gaussian 03 paket programları ile optimize edildi. Moleküler kenetleme çalışmaları için AutoDock 4.2 yazılımı kullanıldı ve kenetleme kompleksleri Discovery Studio Client 4.1 programı kullanılarak 2D ve 3D olarak analiz edildi. Teorik ADMET parametrelerini hesaplamak için pkCSM çevrimiçi programı kullanıldı.

**Sonuç ve Tartışma:** Moleküler kenetleme çalışmaları sonucunda deksrazoksanın B metabolitinin, hem deksrazoksana hem de diğer metabolitlerine kıyasla insan DNA topoizomerez II beta'ya daha fazla bağlanma potansiyeli olduğu belirlendi. Literatürde bildirilen diğer bileşiklerin de insan DNA topoizomerez II beta'ya bağlanma potansiyelleri sırası ile radisikol>kinakrin>purpurin>9-Aminoakridin>heksilresorsinol şeklindeydi.

Sonuçlar, deksrazoksanın antrasiklin kardiyo toksisitesine karşı kardioprotektif etki mekanizmasında deksrazoksanın B metabolitinin önemli bir rol oynadığını göstermiştir. Bunun yanında, araştırılan diğer bileşiklerden purpurin dışındakilerin toksisite oluşturma potansiyelleri olduğu da belirlenmiştir.

**Anahtar Kelimeler:** Antrasiklin kardiyo toksisitesi, deksrazoksana, *in silico* analiz, kardioprotektif ajanlar, topoizomerez II inhibitörleri

## INTRODUCTION

Anthracycline antibiotics (daunorubicin, doxorubicin, epirubicin, idarubicin, mitoxantron) have been widely used for many years in the treatment of solid and hematological tumors [1]. However, their clinical use are limited due to the severe cardiotoxic effects [2-4]. Reducing the cumulative dose of anthracycline is the main approach to preventing the cardiotoxicity, in addition, treatment with dexrazoxane (DEX), the only FDA-approved antidote, is recommended against some anthracycline-related cardiotoxicities and accidental anthracycline extravasation [5-8]. Clinical use of DEX, however, is limited due to concerns that it may increase the myelosuppressive effects of anthracyclines and ifosfamide [9] and it may also cause secondary malignancies after treatment for some pediatric cancers [10,11].

DEX (ICRF-187); is a (S)-4,4'-(1-methyl-1,2-ethanedyl) bis-2,6-piperazinedione and belongs to the bis-dioxopiperazines [12]. It is reported *in vitro* and *in vivo* studies that DEX was biotransformed to an EDTA-like ADR-925 active metabolite via two hydrolytic intermediates (metabolites B and C; Figure 1) [13-15].

Although it is accepted that ADR-925 protects cardiomyocytes by chelating increased intracellular iron as a result of anthracycline-induced oxidative damage, however, compounds that are stronger than DEX in terms of iron-chelating do not have a protective effect or have a less protective effect than DEX against anthracycline cardiotoxicity [15-18]. On the other hand, another mechanism that has come to the fore in recent years regarding the cardioprotective property of DEX is that it may

catalytically inhibit the topoisomerase II beta enzyme (topo II $\beta$ ) in cardiomyocytes [19-24], however, it is not yet known whether DEX or its metabolite(s) exert this inhibition.

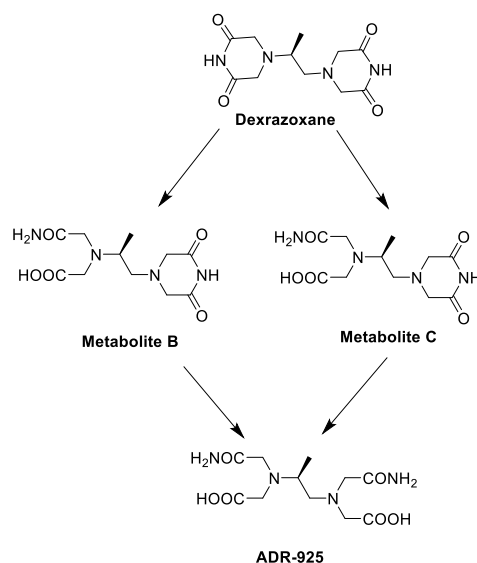


**Figure 1.** Biotransformation of Dexrazoxane (ICRF-187). (The molecular structures were drawn by ChemOffice Suite V20.1.1 software).

In the present study, we focused on the question that which metabolite(s) or DEX itself inhibits topo II $\beta$  and plays a role in the cardioprotective effect. For this purpose, we performed molecular docking studies to determine the interaction of DEX and its three metabolites (Figure 1) with human DNA topoisomerase II alpha (topo II $\alpha$ ) and topo II $\beta$  enzymes. In addition, we also performed the docking studies for topo II $\alpha$  and topo II $\beta$  of five of the reported compounds (Figure 2; hexylresorcinol, purpurin, radicicol, quinacrine, 9-Aminoacridine) to be inhibitors against topo VI, a type of topo II $\beta$ , found in both prokaryotes and some eukaryotes such as plants and algae [25-28]. Finally, we also investigated the some ADMET properties of these five compounds to find nontoxic possible topo II $\beta$  inhibitors as well as the docking studies.

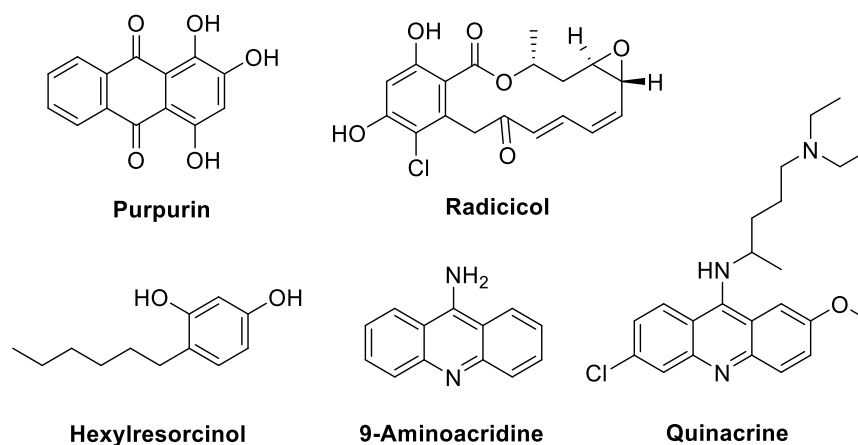


**Figure 2.** Chemical structures of possible five inhibitors of human topo II $\beta$ . (The molecular structures were drawn by ChemOffice Suite V20.1.1 software)

## MATERIAL AND METHOD

### Molecular docking studies of human topo II $\alpha$ and topo II $\beta$ enzymes

Molecular docking studies were conducted using AutoDock 4.2 software to identify the interactions of nine compounds with topo II $\alpha$  and topo II $\beta$ . Crystal structures of human topo II $\alpha$  (PDB ID; 1ZXN) [29] and topo II $\beta$  (PDB ID; 3QX3) [30] were obtained from the RCSB Protein Data Bank ([www.rcsb.org](http://www.rcsb.org)). The molecular structure of the compounds was designed using Gaussview 5.0 and later optimized using the Gaussian 03 package based on the theoretical level of the B3LYP method and the 6–31G basis set. To find potential binding sites between topo II enzymes of the optimized molecular structures, active sites were determined from the interaction map of the ligands, which the enzymes made complexes in the crystal structure and docking studies were performed for the identified active regions.

The validation of molecular docking studies was performed for both topo II $\alpha$  and topo II $\beta$  enzymes. The fact that the Cluster RMSD (Root-mean-square Deviation) value calculated in the docking validation is in the range of 0-2 Å indicates that the docking operation is valid. The docking method was also optimized by re-docking of co-crystallized ligands into the binding site of target proteins. For re-dock method, the native ligands Adenine diphosphate and Etoposide were docked into their binding site on 1ZXN and 3QX3 PDB codes, respectively. The RMSD values of the re-docked ligands were calculated on DockRMSD online software (<https://zhanggroup.org/DockRMSD/>) and RMSD values of the ligands found as 1.951 Å, and 1.352 Å respectively.

In DNA docking studies x: 51.354; y: -3.049; z: 78.946 for topo II $\alpha$ , and x: 26.813; y: 105.382; z: 37.638 for topo II $\beta$  were determined as coordinate centers. Then, using a grid box with 50×50×50 points at the center of the predicted locations and a grid point spacing of 0.375 Å, the lowest placed conformations were selected for further studies. Water molecules were removed with AutoDock tools and subsequently polar hydrogen atoms, Gasteiger partial charges, and Kollman charges were added to the targets. Additionally, the rotatable bonds of the compounds were adjusted. Lamarckian genetic algorithm approach was applied in both simulations. The interactions of topo II $\alpha$  and topo II $\beta$  with the compounds were analyzed using the Discovery Studio Client 4.1 program.

### Theoretical pharmacokinetic study for possible human topo II $\alpha$ and topo II $\beta$ inhibitors

Theoretical some ADMET information of the compounds were also calculated by using the pkCSM program [31]. LogP, Caco-2 permeability, and small intestine absorption represent the lipophilicity, the apparent predicted intestinal permeability, and the percent absorption of the compounds (Intest. Abs.%), respectively. Steady-state volume of distribution (VD<sub>ss</sub>) means drug distribution in the body and the fraction unbound (F<sub>u</sub>) shows portion of free drug in plasma. Excretion of the compounds are predicted via the total clearance (Total C) and whether substrate for kidney OCT2 (organic cation transporter 2). The hERG (the human Ether-à-go-go-Related Gene) I-II inhibition, hepatotoxicity, and skin sensitization represent the toxicity of the compounds.

## RESULT AND DISCUSSION

### Binding affinity of the ligands to topo II $\alpha$ and topo II $\beta$

In the validation of molecular docking of topo II $\alpha$ ; ADP (Adenine diphosphate) ligand with 1ZXN PDB ID code obtained from the protein data bank. The docking was done in the grid box created for the target region. It was determined that the cluster RMSD value of the ligand molecule, which was tested with 10 different conformations, was 1.67 Å°. For topo II $\beta$  validation, Etoposide ligand with 3QX3 PDB ID code obtained from the protein data bank and the docking was done in the grid box created for the target region. The cluster RMSD value of the ligand molecule, which was tested with 10 different conformations, was 0.47 Å°. It was determined that the ligand compounds docking for the determined target region of both enzymes had compatible RMSD values. The clustering histogram and RMSD tables have been added to supplementary information (Suppl. Table 1 and 2).

The binding studies with topo II $\alpha$  and topo II $\beta$  were conducted by docking the compounds with the 1ZXN and 3QX3 crystal structures. The binding energies of the compounds were in the range of -3.47 to -8.22 kcal/mol for topo II $\alpha$ , and -3.75 to -10.77 kcal/mol for topo II $\beta$  (Table 1).

**Table 1.** Docking scores of the compounds with topo II enzymes

Compounds	Topoisomerase II $\alpha$ (PDB ID: 1ZXN)			Topoisomerase II $\beta$ (PDB ID: 3QX3)		
	Binding Energy (kcal/mol)	Ligand efficiency	Inh. con. ( $\mu$ M)	Binding Energy (kcal/mol)	Ligand efficiency	Inh. con. ( $\mu$ M)
DEX	-6.63	-0.35	13.7	-5.88	-0.31	49.36
B	-5.16	-0.26	165.8	-5.66	-0.28	71.27
C	-5.08	-0.25	187.55	-5.46	-0.27	99.8
ADR-925	-3.47	-0.17	2870	-3.75	-0.18	1790
Quinacrine	-6.83	-0.24	9.83	-8.70	-0.31	0.417
9-Aminoacridine	-6.50	-0.43	17.08	-7.21	-0.48	5.22
Purpurin	-7.35	-0.39	4.1	-8.14	-0.43	1.08
Hexylresorcinol	-5.67	-0.41	70.35	-6.30	-0.45	24.09
Radicalol	-8.22	-0.33	0.936	-10.77	-0.43	0.013

The efficiency of the docking conformations of the ligands and the theoretically calculated inhibition concentrations are also shown in Table 1. The results indicated that DEX's metabolites B (Figure 4) and C (Figure 5) have a higher binding affinity for topo II $\beta$  and metabolite B has greater binding affinity than C (Table 1), while DEX itself has a higher binding affinity for topo II $\alpha$  (Table 1, Figure 3). It was also found that other five compounds (hexylresorcinol, purpurin, quinacrine, radicalol, 9-Aminoacridine) have a higher potential to inhibit topo II $\beta$  than topo II $\alpha$ . The binding potentials of these compounds to human topo II $\beta$  were radicalol>quinacrine>purpurin>9-Aminoacridine>hexylresorcinol, respectively (Table 1, Suppl. Figure 6-10).

In addition, 2D interaction of the compounds with the active site in the target enzymes was analyzed to elucidate their interactions. Hydrogen bonding and other non-covalent interactions are

shown in Table 2. It was found that the compounds generally form H-bonds with ALA167, ASN91, SER148, and non-covalent interactions with ILE141, PHE142, and MG900 in 2D interactions with topo II $\alpha$ . These amino acids are the interacting residues of the topo II $\alpha$  in their complex with the ADP ligand [29]. On the other hand, it was found that the compounds generally form H-bonds with ASP479, ARG503, and non-covalent interactions with ARG503, DC8, and DT9 in 2D interactions of the compounds with topo II $\beta$ .

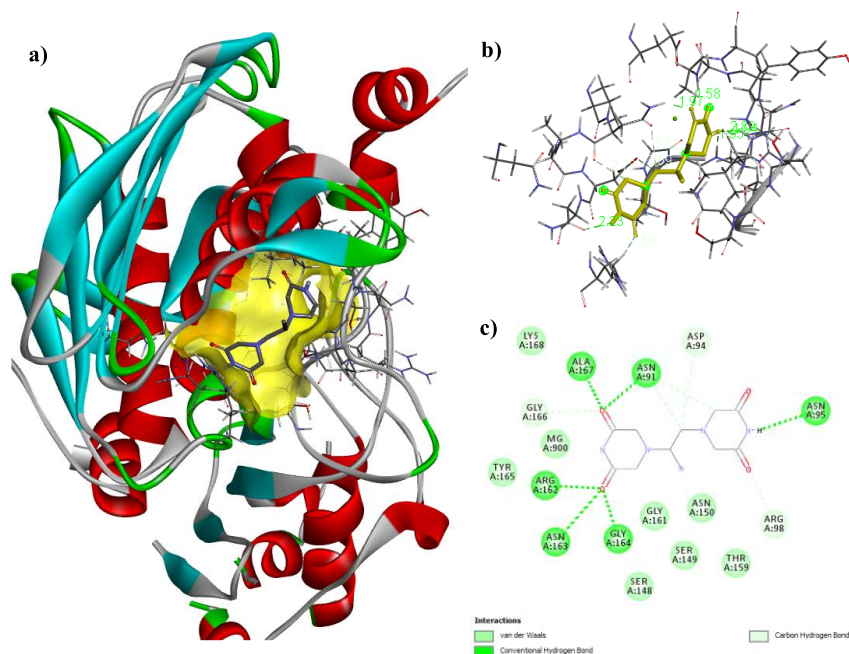


**Figure 3.** The 3D and 2D docking mode of DEX with topo II $\alpha$  (PDB ID:1ZXN). a) 3D structure of the enzyme-ligand complex b) 3D ligand interactions c) 2D ligand interactions (Note :a, b, and c indicate the same expressions in figures 4 and 5).

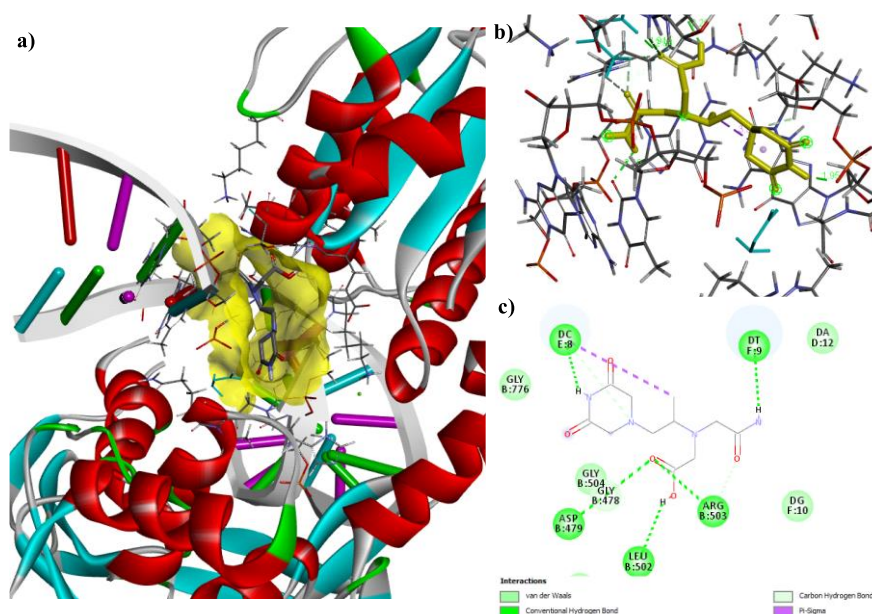


**Figure 4.** The 3D and 2D docking mode of metabolite B with topo II $\beta$  (PDB ID:3QX3).

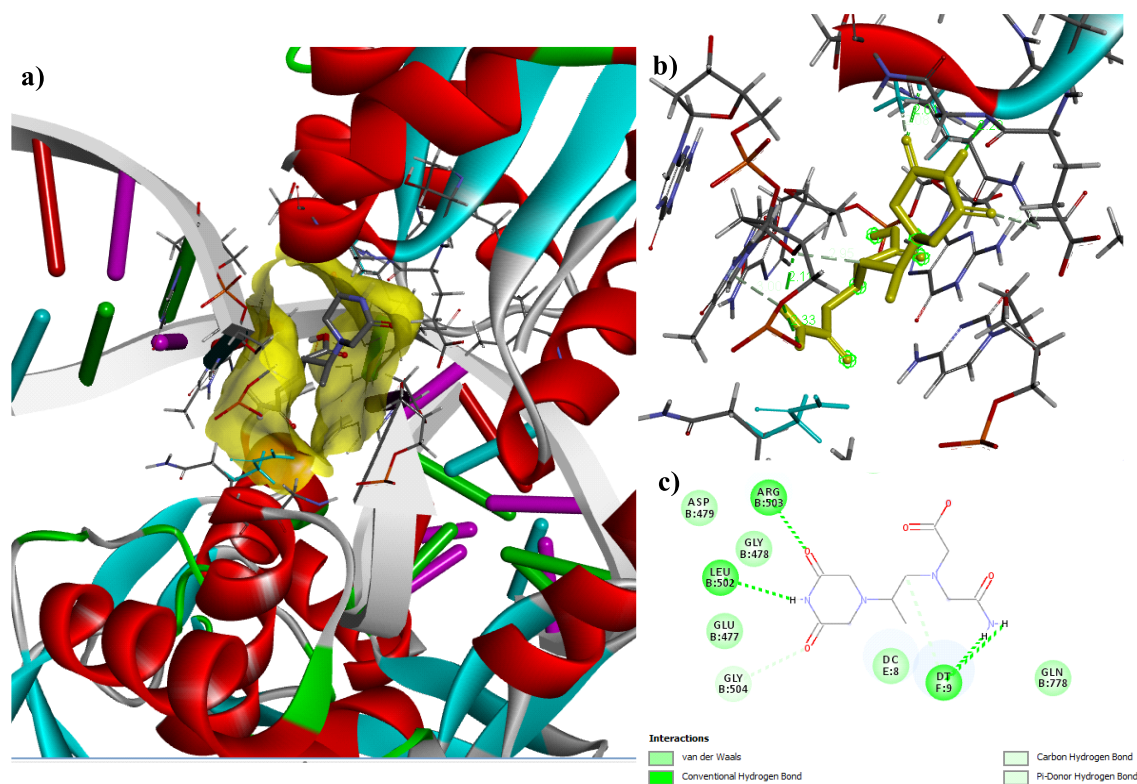


**Figure 5.** The 3D and 2D docking mode of metabolite C with topo II $\beta$  (PDB ID:3QX3).

### ADMET properties of the compounds that are potential human topo II inhibitors

The results of some ADMET parameters (Caco-2 permeability, intestinal absorption, VDss, Fu, total C, the substrate for kidney OCT2, hERG I/II inhibition, hepatotoxicity, skin sensitization) of the compounds are shown in Table 3.

According to the ADMET results, the log P values of the compounds, except for quinacrine, seem to comply with Lipinski rules [32]. The obtained results showed that hexylresorcinol, quinacrine, radicicol, and 9-aminoacridine have suitable for Caco-2 permeability. DEX and purpurin seem like Caco-2 impermeable however their intestinal absorption was 51% and 73%, respectively (less than 30% indicates poor absorption). Intestinal absorptions of the other four compounds ranged from 81% to 95% (Table 3).

The results from the theoretical distribution of the compounds in the body (VDss) showed that they, except for DEX, are found in plasma rather than in tissues (VDss is considered low if it is <0.15 and high if it is >0.45). In this context, the Fu values (indicate the free fraction of the compounds in plasma) of the compounds other than DEX were found to be low which means that the compounds' binding rates to plasma proteins increase (Table 3).

**Table 2.** Docking interactions of the compounds with human topo II enzymes

Compounds	Topoisomerase II $\alpha$ (PDB ID: 1ZXX)		Topoisomerase II $\beta$ (PDB ID: 3QX3)	
	H-bonding	Other non-covalent interactions	H-bonding	Other non-covalent interactions
<b>DEX</b>	ALA167, ASN91, ASN95, ARG162, ASN163, GLY164,	ARG98, GLY166, ASP94	ASP479, GLN778, DC8	DC8, ARG503, GLY478
<b>B</b>	ASN120, ILE141, ASP94, ASN91, ALA167	PHE142, ILE141, ASN91, MG900	DC8, DT9, ASP479, ARG503, LEU502	DC8
<b>C</b>	LYS168, ALA167, ILE141, ASN163, GLY164, ARG162, ASN91	GLY161, MG900	ARG503, LEU502, DT9	GLY504, DT9
<b>ADR-925</b>	SER148, SER149, LYS168, ALA167, GLY164, ILE141, ASN163, ARG162	MG900, ASN91, THR147	DC8, DG10, DT9, ARG503, ASP479	DT9, GLY504
<b>Hexylresorcinol</b>	SER148, ARG162, ASN91, ALA167	ILE141, PHE142, MG900, GLY166	DT9, ASP479	DG13, DA12, ARG503, GLY478
<b>Purpurin</b>	ALA167, ASN91, GLU87, SER149, SER148, ASN150	ILE141, PHE142, LYS168, MG900	DG10, ASP479, DC8	ARG503, SER480
<b>Quinacrine</b>	ASN91	ALA92, ALA167, ILE141, ILE125, ARG98	ARG503	DT9, DG13, DA12, DC8
<b>Radicol</b>	LYS168, GLY161, ASP94	PHE142, ALA167, ARG98	ASP479	DA12, DG13, ARG503, DC8, DG10
<b>9-Aminoacridine</b>	ASN91, ALA167, SER148	MG900, LYS168, PHE142, ILE141	ASP479, DT9	ARG503, DT9

The clearance results suggested that the compounds were not substrate for OCT2, which is a renal transporter that plays an important role in the disposition and renal clearance of xenobiotics and endogenous compounds. Total clearance of the compounds was between 0.056 and 1.099 log mL/min/kg (Table 3).

Another important ADMET parameter for xenobiotics is the inhibition of hERG because it encodes a subunit of a potassium ion channel which regulates the cardiac action potential. Inhibition of hERG can lead to acquiring long QT syndrome and fatal ventricular arrhythmia [33]. The results indicated that the compounds, except for quinacrine, do not inhibit hERG I/II. In addition, according to other theoretical toxicity results, radicol and quinacrine can potentially cause hepatotoxicity, while 9-aminoacridine and hexylresorcinol can produce skin sensitization. On the other hand, purpurin theoretically does not cause any toxicity (Table 3).

### Possible cardioprotective mechanism of DEX

In recent years, it has been suggested that DEX's cardioprotective mechanism depends on inhibiting topo II $\beta$ , which is expressed higher than topo II $\alpha$  in the heart, rather than chelates increased free iron by oxidative stress in cardiomyocytes caused by anthracycline treatment [15-24]. Since DEX is administered at the clinic as an intravenous infusion, it is rapidly distributed to the heart and then to

the whole body. VD<sub>ss</sub> and Fu results also showed that DEX can be found in tissues rather than plasma after the treatment. An *in vivo* study was shown that DEX reaches the heart and it is biotransformed into its metabolites B, C and ADR-925 [15]. Similar biotransformation results were also obtained from *in vitro* studies [13, 14]. The biotransformation of DEX to a large extent in the heart rather than the liver may play a role in the cardioprotective effect because one or two its metabolite(s) may inhibit the topo II $\beta$ . The molecular docking studies indicated that DEX has a greater binding affinity for topo II $\alpha$  (Figure 3) while its metabolites (B and C) to topo II $\beta$  (Table 1, Figure 4, and 5). In addition, DEX's ADR-925 metabolite, which is reported to play main role in the cardioprotective effect by chelating increased iron, had a low binding affinity for both topo II $\alpha$  (Table 1, Suppl. Figure 4) and topo II $\beta$  (Table 1, Suppl. Figure 5). As the B metabolite of DEX has a greater binding affinity to topo II $\beta$  (Figure 4) than topo II $\alpha$  (Suppl. Figure 2) and theoretically inhibits the enzyme at lower concentrations (IC: 71.27  $\mu$ M) by comparison the C metabolite of DEX (IC: 99.8  $\mu$ M), the B metabolite of DEX may play a role in the cardioprotective effect against anthracycline-induced cardiotoxicity.

**Table 3.** Theoretical pharmacokinetic study for ADMET properties

Compounds	Log P	Caco2 permeability	Human intestinal abs. (%)	VD <sub>ss</sub> (human)	Fu (human)	Total C (log mL/min/kg)	Renal OCT2 Substrate	hERG I/II	Hepatotoxicity	Skin Sensitive
DEX	-2.70	-0.089	51	-0.17	0.89	0.972	No	No	No	No
Purpurin	1.58	-0.32	73	0.11	0.16	0.056	No	No	No	No
Radicicol	2.69	1.103	83	0.24	0.297	0.321	No	No	Yes	No
Quinacrine	5.97	1.00	91	1.71	0.124	1.099	No	I-No, II-Yes	Yes	No
9-Aminoacridine	2.97	1.31	95	0.25	0.17	0.613	No	No	No	Yes
Hexylresorcinol	3.22	1.33	91	0.37	0.357	0.349	No	No	No	Yes

### Probable and nontoxic human topo II $\beta$ inhibitors

The compounds reported in the literature to be inhibitors (hexylresorcinol, purpurin, quinacrine, radicol, and 9-Aminoacridine) for topo VI, a prototypical topo II $\beta$ , were also investigated whether it would inhibit human topo II $\beta$ . Because both some recent publications [19-24], and our results suggested that inhibition of topo II $\beta$  plays a key role in the cardioprotective effect of DEX. On the other hand, since DEX has limited clinical use due to some adverse effects [10, 11], theoretical toxicities of these compounds were also investigated to determine whether they could be an alternative to DEX. Although radicol and quinacrine are the first two compounds with the highest binding affinity to topo II $\beta$  among alternative compounds, they have the potential to produce hepatotoxicity and quinacrine can also induce cardiotoxicity by inhibiting hERG I/II according to our *in silico* ADMET results. Human hepatotoxicity of quinacrine was also reported in the literature [35, 36], but there is no study related to cardiotoxicity. No toxicity has been reported with radicol either. In contrast, it has been reported to ameliorate

crotoxin-damaged skeletal muscle in mice [37, 38]. On the other hand, purpurin, which is the third highest binding potential to human topo II $\beta$ , does not cause any toxicity and it inhibits human topo II $\beta$  at a low concentration of 1.08  $\mu$ M (Table 1). At the same time, there is no report related to purpurin toxicity. On the contrary, *in vitro*, and *in vivo* studies have been reported that it has antioxidant, antimicrobial, anticancer, and neuroprotective effects [39]. 9-aminoacridine and hexylresorcinol, which have less binding affinity for topo II $\beta$  than the other compounds, are also likely to cause toxicity (skin sensitization, Table 3). This toxic effect has also been reported in a case report [40].

The results of the *in silico* study showed that metabolite B plays a role in the cardioprotective mechanism of action of DEX by inhibiting topo II $\beta$ . It has also shown that the compounds previously known to be inhibitors of topo VI may be inhibitors of both human topo II enzymes at lower concentrations compared to both DEX and its metabolites. Based on our results, compounds other than purpurin are likely to cause toxicity. On the other hand, no toxicity of purpurin was observed in this study and also in the literature according to the literature search carried out until March 10.

## AUTHORS CONTRIBUTIONS

Conception: F.K.; Design: F.K., B.K.; Supervision: F.K.; Resources: F.K., B.K.; Materials: B.K.; Data Collection and/or processing: B.K., F.K.; Analysis and/or interpretation: B.K., F.K.; Literature search: F.K., B.K.; Writing manuscript: F.K., B.K.; Critical review: F.K., B.K.; Other: -

## CONFLICT OF INTEREST

The authors declare that there are no actual, potential or perceived conflicts of interest.

## ETHICS COMMITTEE APPROVAL

The authors declare that ethics committee approval is not required for this study

## REFERENCES

1. Minotti, G., Menna, P., Salvatorelli, E., Cairo, G., Gianni, L. (2004). Anthracyclines: molecular advances and pharmacologic developments in antitumor activity and cardiotoxicity. *Pharmacological Reviews*, 56(2), 185–229. [\[CrossRef\]](#)
2. Lefrak, E. A., Pitha, J., Rosenheim, S., Gottlieb, J. A. (1973). A clinicopathologic analysis of adriamycin cardiotoxicity. *Cancer*, 32(2), 302–314. [\[CrossRef\]](#)
3. Gerber, M. A., Gilbert, E. M., Chung, K. J. (1975). Adriamycin cardiotoxicity in a child with Wilms tumor. Report of a case and review of the literature. *The Journal of Pediatrics*, 87(4), 629–632. [\[CrossRef\]](#)

4. McGowan, J. V., Chung, R., Maulik, A., Piotrowska, I., Walker, J. M., Yellon, D. M. (2017). Anthracycline Chemotherapy and Cardiotoxicity. *Cardiovascular Drugs and Therapy*, 31(1), 63–75. [[CrossRef](#)]
5. Von Hoff, D. D., Layard, M. W., Basa, P., Davis, H. L., Jr, Von Hoff, A. L., Rozenzweig, M., Muggia, F.M. (1979). Risk factors for doxorubicin-induced congestive heart failure. *Annals of Internal Medicine*, 91(5), 710–717. [[CrossRef](#)]
6. Wouters, K. A., Kremer, L. C., Miller, T. L., Herman, E. H., Lipshultz, S. E. (2005). Protecting against anthracycline-induced myocardial damage: a review of the most promising strategies. *British Journal of Haematology*, 131(5), 561–578. [[CrossRef](#)]
7. Hasinoff, B. B. (2006). Dexrazoxane use in the prevention of anthracycline extravasation injury. *Future Oncology* (London, England), 2(1), 15–20. [[CrossRef](#)]
8. Speyer, J. L., Green, M. D., Kramer, E., Rey, M., Sanger, J., Ward, C., Dubin, N., Ferrans, V., Stecy, P., Zeleniuch-Jacquotte, A. (1988). Protective effect of the bispiperazinedione ICRF-187 against doxorubicin-induced cardiac toxicity in women with advanced breast cancer. *The New England Journal of Medicine*, 319(12), 745–752. [[CrossRef](#)]
9. Spalato Ceruso, M., Napolitano, A., Silletta, M., Mazzocca, A., Valeri, S., Improta, L., Santini, D., Tonini, G., Badalamenti, G., Vincenzi, B. (2019). Use of Cardioprotective Dexrazoxane Is Associated with Increased Myelotoxicity in Anthracycline-Treated Soft-Tissue Sarcoma Patients. *Chemotherapy*, 64(2), 105–109. [[CrossRef](#)]
10. Vrooman, L. M., Neuberg, D. S., Stevenson, K. E., Asselin, B. L., Athale, U. H., Clavell, L., Cole, P. D., Kelly, K. M., Larsen, E. C., Laverdière, C., Michon, B., Schorin, M., Schwartz, C. L., Cohen, H. J., Lipshultz, S. E., Silverman, L. B., Sallan, S. E. (2011). The low incidence of secondary acute myelogenous leukaemia in children and adolescents treated with dexrazoxane for acute lymphoblastic leukaemia: a report from the Dana-Farber Cancer Institute ALL Consortium. *European Journal of Cancer*, 47(9), 1373–1379. [[CrossRef](#)]
11. Walker, D. M., Fisher, B. T., Seif, A. E., Huang, Y. S., Torp, K., Li, Y., Aplenc, R. (2013). Dexrazoxane use in pediatric patients with acute lymphoblastic or myeloid leukemia from 1999 and 2009: analysis of a national cohort of patients in the Pediatric Health Information Systems database. *Pediatric Blood and Cancer*, 60(4), 616–620. [[CrossRef](#)]
12. Hellmann, K, Rhomberg, W. Razoxane and Dexrazoxane – Two Multifunctional Agents: Experimental and Clinical Results, Springer, London, (2010).
13. Hasinoff, B. B. (1989). The interaction of the cardioprotective agent ICRF-187 [(+)-1,2-bis(3,5-dioxopiperazinyl-1-yl)propane]; its hydrolysis product (ICRF-198); and other chelating agents with the Fe(III) and Cu(II) complexes of adriamycin. *Agents and Actions*, 26(3-4), 378–385. [[CrossRef](#)]
14. Hasinoff, B. B., Venkataram, S., Singh, M., Kuschak, T.I. (1994). Metabolism of the cardioprotective agents dexrazoxane (ICRF-187) and levrazoxane (ICRF-186) by the isolated hepatocyte. *Xenobiotica; the Fate of Foreign Compounds in Biological Systems*, 24(10), 977–987. [[CrossRef](#)]
15. Jirkovský, E., Jirkovská, A., Bureš, J., Chládek, J., Lenčová, O., Stariat, J., Pokorná, Z., Karabanovich, G., Roh, J., Brázdová, P., Šimůnek, T., Kovaříková, P., Štěrba, M. (2018). Pharmacokinetics of the Cardioprotective Drug Dexrazoxane and Its Active Metabolite ADR-925 with Focus on Cardiomyocytes and the Heart. *The Journal of Pharmacology and Experimental Therapeutics*, 364(3), 433–446. [[CrossRef](#)]

16. Hasinoff, B. B., Hellmann, K., Herman, E. H., Ferrans, V. J. (1998). Chemical, biological and clinical aspects of dexrazoxane and other bisdioxopiperazines. *Current Medicinal Chemistry*, 5(1), 1-28.
17. Šimůnek, T., Klimentová, I., Kaplanová, J., Sterba, M., Mazurová, Y., Adamcová, M., Hrdina, R., Gersl, V., Ponka, P. (2005). Study of daunorubicin cardiotoxicity prevention with pyridoxal isonicotinoyl hydrazone in rabbits. *Pharmacological Research*, 51(3), 223–231. [\[CrossRef\]](#)
18. Sterba, M., Popelová, O., Šimunek, T., Mazurová, Y., Potáčová, A., Adamcová, M., Kaiserová, H., Ponka, P., Gersl, V. (2006). Cardioprotective effects of a novel iron chelator, pyridoxal 2-chlorobenzoyl hydrazone, in the rabbit model of daunorubicin-induced cardiotoxicity. *The Journal of Pharmacology and Experimental Therapeutics*, 319(3), 1336–1347. [\[CrossRef\]](#)
19. Lyu, Y. L., Kerrigan, J. E., Lin, C. P., Azarova, A. M., Tsai, Y. C., Ban, Y., Liu, L. F. (2007). Topoisomerase II $\beta$  mediated DNA double-strand breaks: implications in doxorubicin cardiotoxicity and prevention by dexrazoxane. *Cancer Research*, 67(18), 8839–8846. [\[CrossRef\]](#)
20. Deng, S., Yan, T., Jendry, C., Nemecek, A., Vincetic, M., Gödtel-Armbrust, U., Wojnowski, L. (2014). Dexrazoxane may prevent doxorubicin-induced DNA damage via depleting both topoisomerase II isoforms. *BMC Cancer*, 14, 842. [\[CrossRef\]](#)
21. Vejpongsa, P., Yeh, E. T. (2014). Topoisomerase 2 $\beta$ : a promising molecular target for primary prevention of anthracycline-induced cardiotoxicity. *Clinical Pharmacology and Therapeutics*, 95(1), 45–52. [\[CrossRef\]](#)
22. Hasinoff, B. B., Patel, D., Wu, X. (2020). The Role of Topoisomerase II $\beta$  in the Mechanisms of Action of the Doxorubicin Cardioprotective Agent Dexrazoxane. *Cardiovascular Toxicology*, 20(3), 312–320. [\[CrossRef\]](#)
23. Hasinoff, B. B., Patel, D., Wu, X. (2020). A QSAR study that compares the ability of bisdioxopiperazine analogs of the doxorubicin cardioprotective agent dexrazoxane (ICRF-187) to protect myocytes with DNA topoisomerase II inhibition. *Toxicology and Applied Pharmacology*, 399, 115038. [\[CrossRef\]](#)
24. Jirkovský, E., Jirkovská, A., Bavlovič-Piskáčková, H., Skalická, V., Pokorná, Z., Karabanovich, G., Kollárová-Brázdová, P., Kubeš, J., Lenčová-Popelová, O., Mazurová, Y., Adamcová, M., Lyon, A. R., Roh, J., Šimůnek, T., Štěrbová-Kovaříková, P., Štěrba, M. (2021). Clinically Translatable Prevention of Anthracycline Cardiotoxicity by Dexrazoxane Is Mediated by Topoisomerase II Beta and Not Metal Chelation. *Circulation: Heart Failure*, 14(11), e008209. [\[CrossRef\]](#)
25. Gabelle, D., Bocs, C., Graille, M., Forterre, P. (2005). Inhibition of archaeal growth and DNA topoisomerase VI activities by the Hsp90 inhibitor radicicol. *Nucleic Acids Research*, 33(7), 2310–2317. [\[CrossRef\]](#)
26. Taylor, J. A., Mitchenall, L. A., Rejzek, M., Field, R. A., Maxwell, A. (2013). Application of a novel microtitre plate-based assay for the discovery of new inhibitors of DNA gyrase and DNA topoisomerase VI. *PloS one*, 8(2), e58010. [\[CrossRef\]](#)
27. Bergerat, A., Gabelle, D., Forterre, P. (1994). Purification of a DNA topoisomerase II from the hyperthermophilic archaeon *Sulfolobus shibatae*. A thermostable enzyme with both bacterial and eucaryal features. *The Journal of Biological Chemistry*, 269(44), 27663–27669. [\[CrossRef\]](#)

28. Sugimoto-Shirasu, K., Stacey, N. J., Corsar, J., Roberts, K., McCann, M. C. (2002). DNA topoisomerase VI is essential for endoreduplication in Arabidopsis. *Current Biology:CB*, 12(20), 1782–1786. [\[CrossRef\]](#)
29. Wei, H., Ruthenburg, A. J., Bechis, S. K., Verdine, G. L. (2005). Nucleotide-dependent domain movement in the ATPase domain of a human type IIA DNA topoisomerase. *The Journal of Biological Chemistry*, 280(44), 37041–37047. [\[CrossRef\]](#)
30. Wu, C. C., Li, T. K., Farh, L., Lin, L.Y., Lin, T. S., Yu, Y. J., Yen, T. J., Chiang, C. W., Chan, N. L. (2011). Structural basis of type II topoisomerase inhibition by the anticancer drug etoposide. *Science* (New York, N.Y.), 333(6041), 459–462. [\[CrossRef\]](#)
31. Pires, D. E., Blundell, T. L., Ascher, D. B. (2015). pkCSM: Predicting Small-Molecule Pharmacokinetic and Toxicity Properties Using Graph-Based Signatures. *Journal of Medicinal Chemistry*, 58(9), 4066–4072. [\[CrossRef\]](#)
32. Lipinski, C. A., Lombardo, F., Dominy, B. W., Feeney, P. J. (2001). Experimental and computational approaches to estimate solubility and permeability in drug discovery and development settings. *Advanced Drug Delivery Reviews*, 46(1-3), 3–26. [\[CrossRef\]](#)
33. Sanguinetti, M. C., Tristani-Firouzi, M. (2006). hERG potassium channels and cardiac arrhythmia. *Nature*, 440(7083), 463–469. [\[CrossRef\]](#)
34. Gadelle, D., Graille, M., Forterre, P. (2006). The HSP90 and DNA topoisomerase VI inhibitor radicicol also inhibits human type II DNA topoisomerase. *Biochemical Pharmacology*, 72(10), 1207–1216. [\[CrossRef\]](#)
35. Gibb, W., Isenberg, D. A., Snaith, M. L. (1985). Mepacrine induced hepatitis. *Annals of the Rheumatic Diseases*, 44(12), 861–862. [\[CrossRef\]](#)
36. Scoazec, J. Y., Krolak-Salmon, P., Casez, O., Besson, G., Thobois, S., Kopp, N., Perret-Liaudet, A., Streichenberger, N. (2003). Quinacrine-induced cytolytic hepatitis in sporadic Creutzfeldt-Jakob disease. *Annals of Neurology*, 53(4), 546–547. [\[CrossRef\]](#)
37. Conte, T. C., Franco, D. V., Baptista, I. L., Bueno, C. R., Jr, Selistre-de-Araújo, H. S., Brum, P. C., Moriscot, A. S., Miyabara, E. H. (2008). Radicicol improves regeneration of skeletal muscle previously damaged by crotoxin in mice. *Toxicon: Official Journal of the International Society on Toxinology*, 52(1), 146–155. [\[CrossRef\]](#)
38. Nascimento, T. L., Conte, T. C., Rissato, T. S., Luna, M. S., Soares, A. G., Moriscot, A. S., Yamanouye, N., Miyabara, E. H. (2019). Radicicol enhances the regeneration of skeletal muscle injured by crotoxin via decrease of NF-kB activation. *Toxicon: official journal of the International Society on Toxinology*, 167, 6–9. [\[CrossRef\]](#)
39. Singh, J., Hussain, Y., Luqman, S., Meena, A. (2020). Purpurin: A natural anthraquinone with multifaceted pharmacological activities. *Phytotherapy Research:PTR*, 10.1002/ptr.6965. Advance online publication. [\[CrossRef\]](#)
40. Burrows, D., Irvine, J. (1982). Contact dermatitis to hexylresorcinol. *Contact Dermatitis*, 8(1), 71. [\[CrossRef\]](#)

## **SUPPLEMENTARY MATERIAL**

**Table 1.** The cluster histogram and RMSD table for topo II $\alpha$  (PDB ID: 1ZZN)

CLUSTERING HISTOGRAM												
Clus-ter Rank	Lowest Binding Energy	Run	Mean Binding Energy	Num in Clus	Histogram							
					5	10	15	20	25	30	35	
1	-8.37	9	-8.37	1	#							
2	-8.33	6	-7.90	8	#####							
3	-7.93	3	-7.93	1	#							

Number of multi-member conformational clusters found = 1, out of 10 runs.

RMSD TABLE						
Rank	Sub-Rank	Run	Binding Energy	Cluster RMSD	Reference RMSD	Grep Pattern
1	1	9	-8.37	0.00	3.13	RANKING
2	1	6	-8.33	0.00	1.54	RANKING
2	2	4	-8.13	1.76	2.21	RANKING
2	3	10	-8.05	1.67	0.99	RANKING
2	4	2	-8.01	1.85	1.74	RANKING
2	5	7	-7.96	1.85	2.47	RANKING
2	6	8	-7.94	1.58	1.62	RANKING
2	7	1	-7.61	1.66	1.91	RANKING
2	8	5	-7.21	1.75	1.55	RANKING
3	1	3	-7.93	0.00	2.85	RANKING

**Table 2.** The cluster histogram and RMSD table for topo II $\beta$  (PDB ID: 3QX3)

CLUSTERING HISTOGRAM												
Clus-ter Rank	Lowest Binding Energy	Run	Mean Binding Energy	Num in Clus	Histogram							
					5	10	15	20	25	30	35	
1	-13.58	4	-13.39	8	#####							
2	-12.55	1	-12.48	2	##							

Number of multi-member conformational clusters found = 2, out of 10 runs.

RMSD TABLE						
Rank	Sub-Rank	Run	Binding Energy	Cluster RMSD	Reference RMSD	Grep Pattern
1	1	4	-13.58	0.00	16.73	RANKING
1	2	9	-13.54	0.12	16.72	RANKING
1	3	5	-13.53	0.17	16.70	RANKING
1	4	3	-13.52	0.27	16.68	RANKING
1	5	2	-13.52	0.27	16.69	RANKING
1	6	7	-13.49	0.31	16.74	RANKING
1	7	10	-13.43	0.47	16.57	RANKING
1	8	8	-12.50	1.58	16.61	RANKING
2	1	1	-12.55	0.00	16.38	RANKING
2	2	6	-12.40	1.10	16.39	RANKING

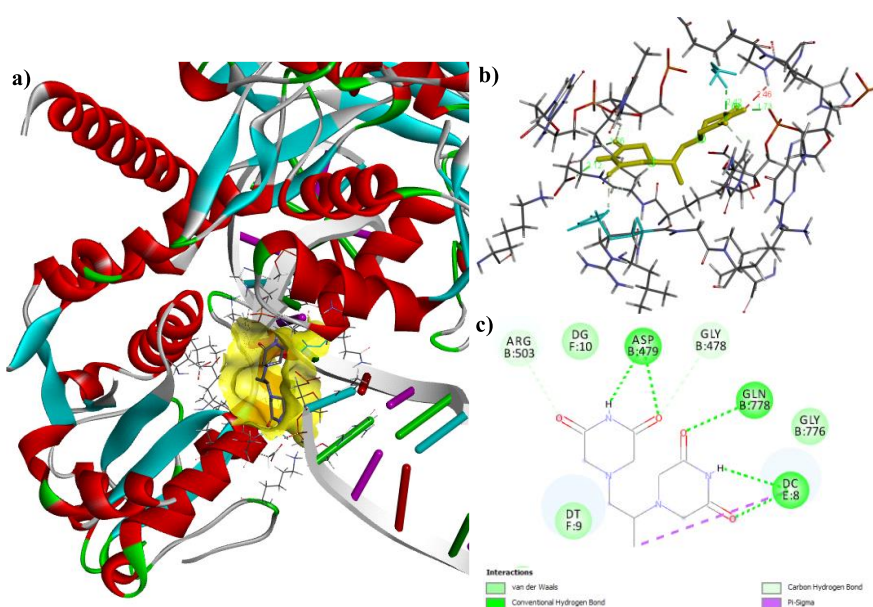


**Figure 1.** The 3D and 2D docking mode of DEX with topo II $\beta$  (PDB ID:3QX3). a) 3D structure of the enzyme-ligand complex b) 3D ligand interactions c) 2D ligand interactions (Note :a, b, and c indicate the same expressions from figures 2 to 10)

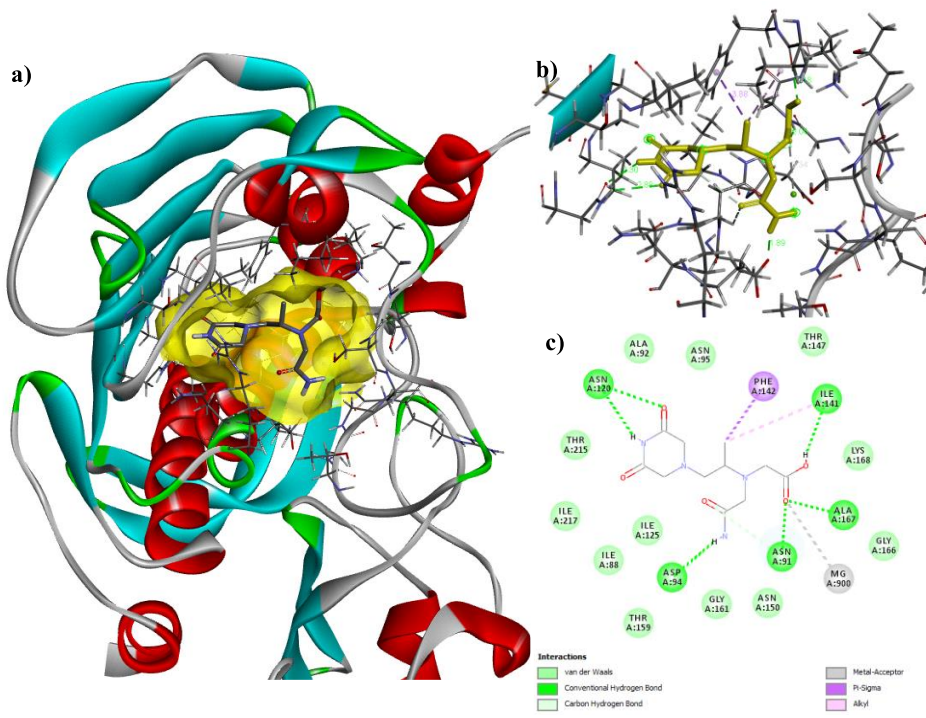


**Figure 2.** The 3D and 2D docking mode of metabolite B with topo II $\alpha$  (PDB ID:1ZXN).

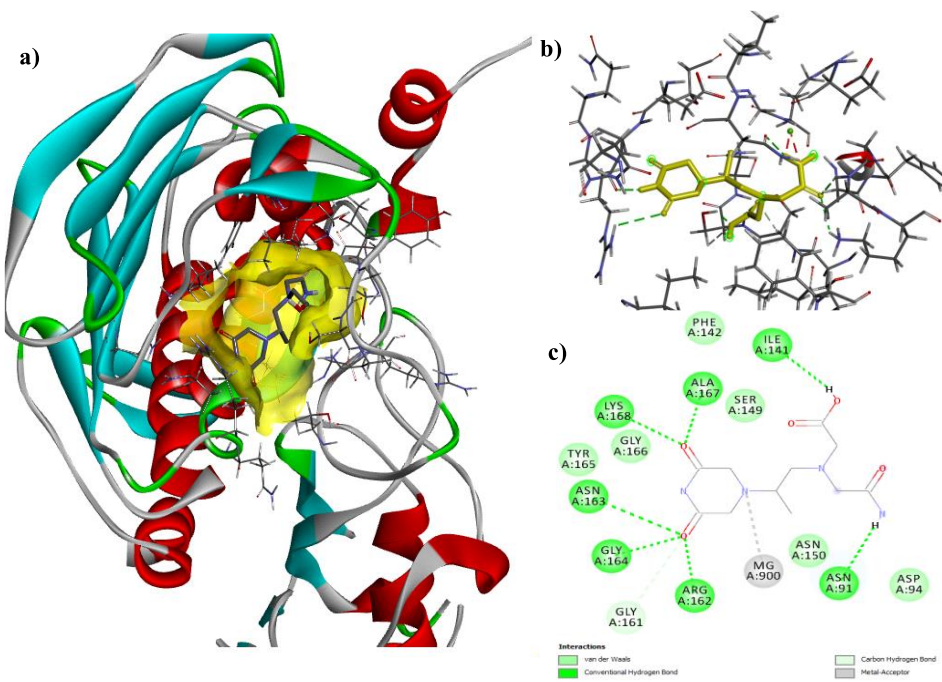


**Figure 3.** The 3D and 2D docking mode of metabolite C with topo II $\alpha$  (PDB ID:1ZXN).

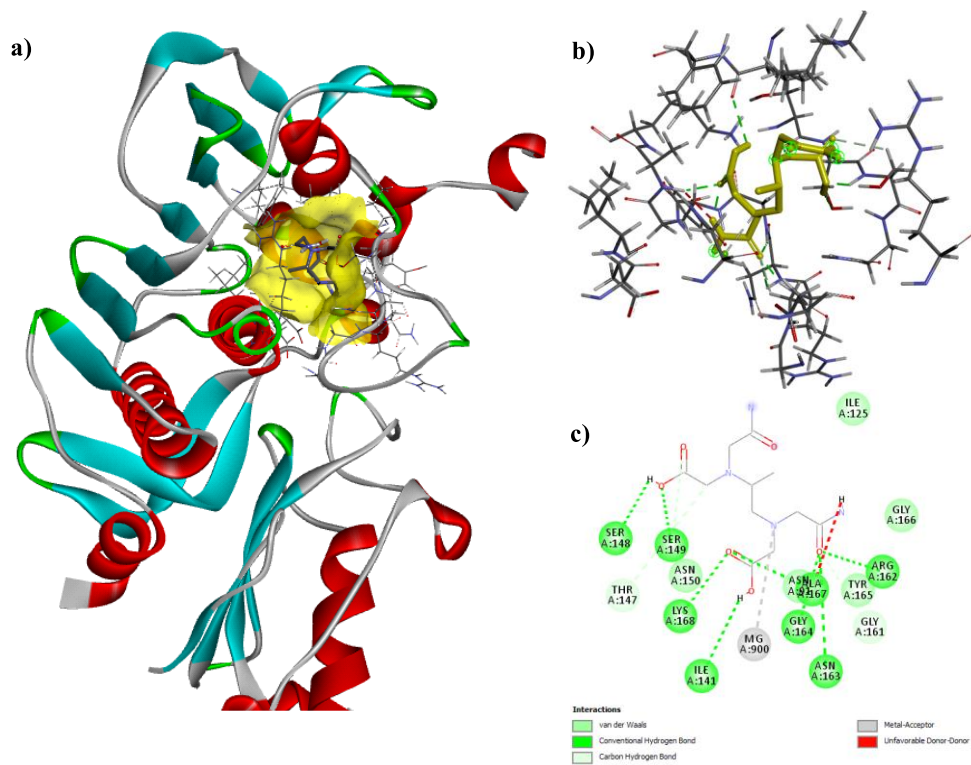


**Figure 4.** The 3D and 2D docking mode of metabolite ADR-925 with topo II $\alpha$  (PDB ID:1ZXN).

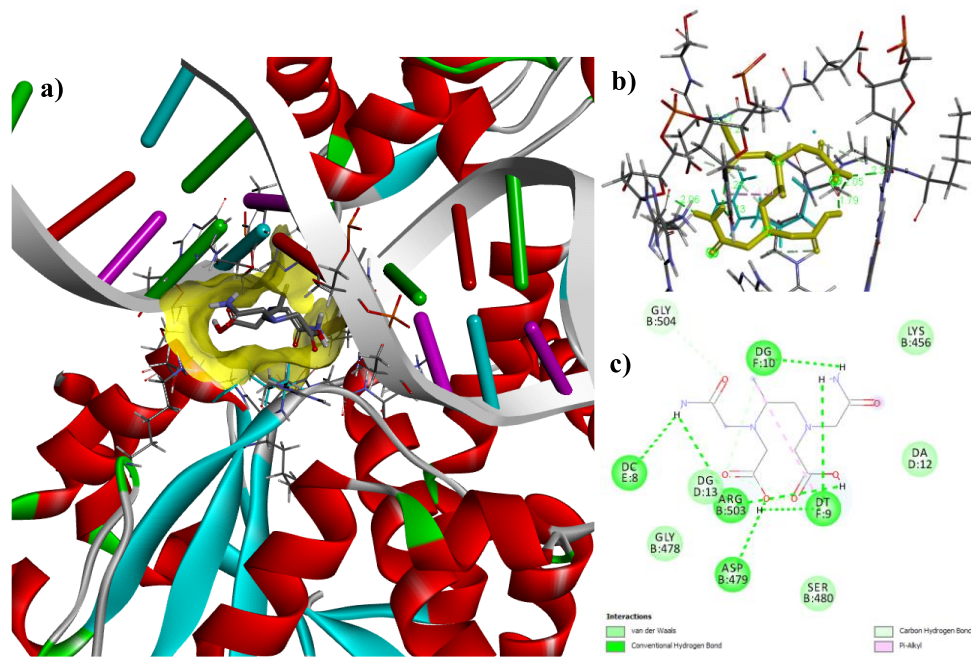


**Figure 5.** The 3D and 2D docking mode of metabolite ADR-925 with topo II $\beta$  (PDB ID:3QX3).

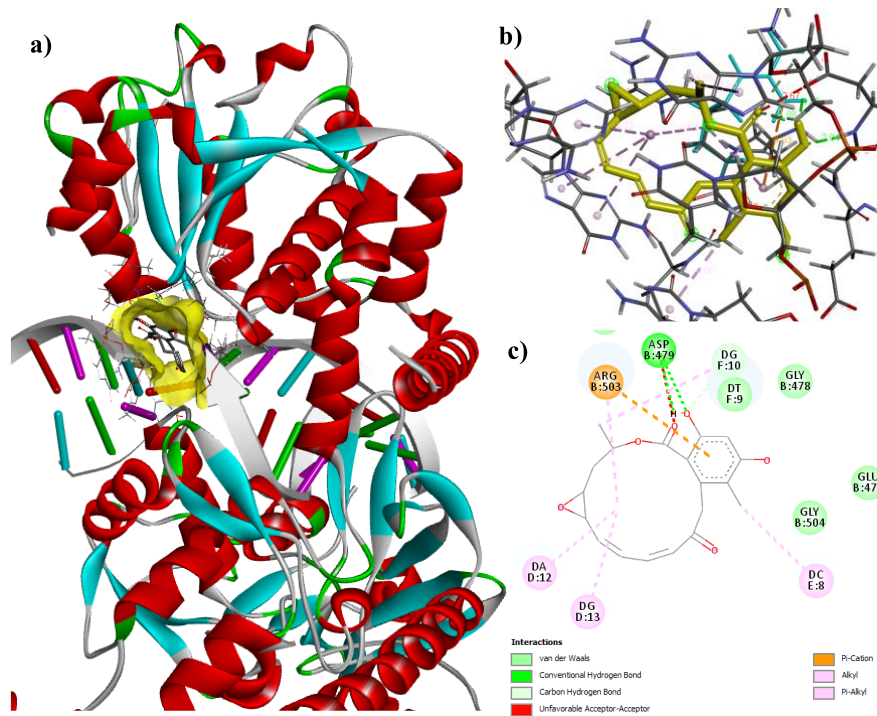


**Figure 6.** The 3D and 2D docking mode of radical with topo II $\beta$  (PDB ID:3QX3).

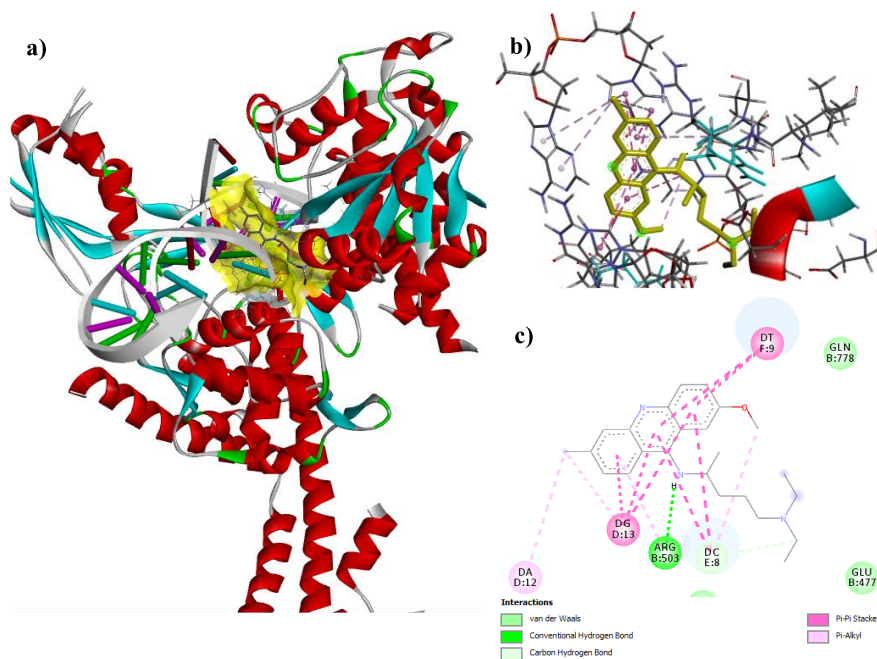


**Figure 7.** The 3D and 2D docking mode of quinacrine with topo II $\beta$  (PDB ID:3QX3).

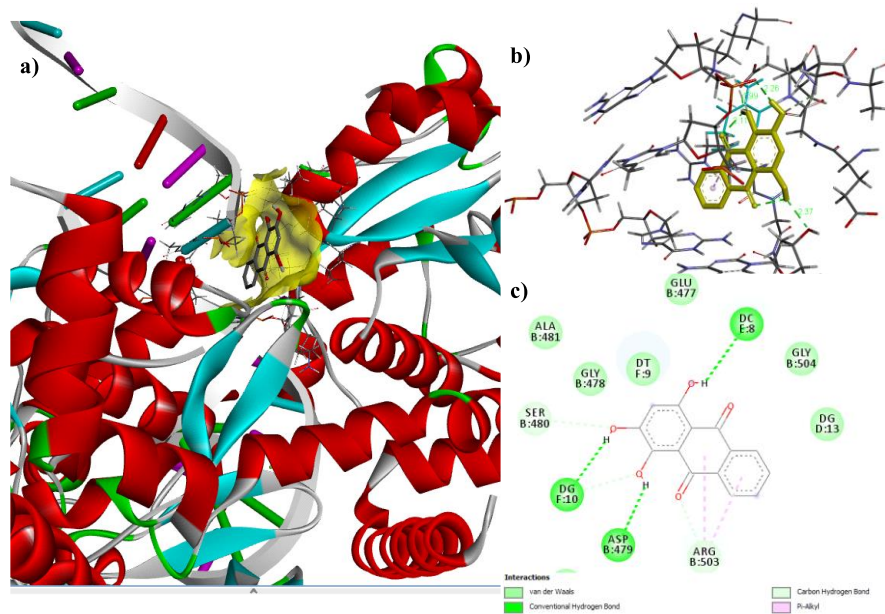


**Figure 8.** The 3D and 2D docking mode of purpurine with topo II $\beta$  (PDB ID:3QX3).

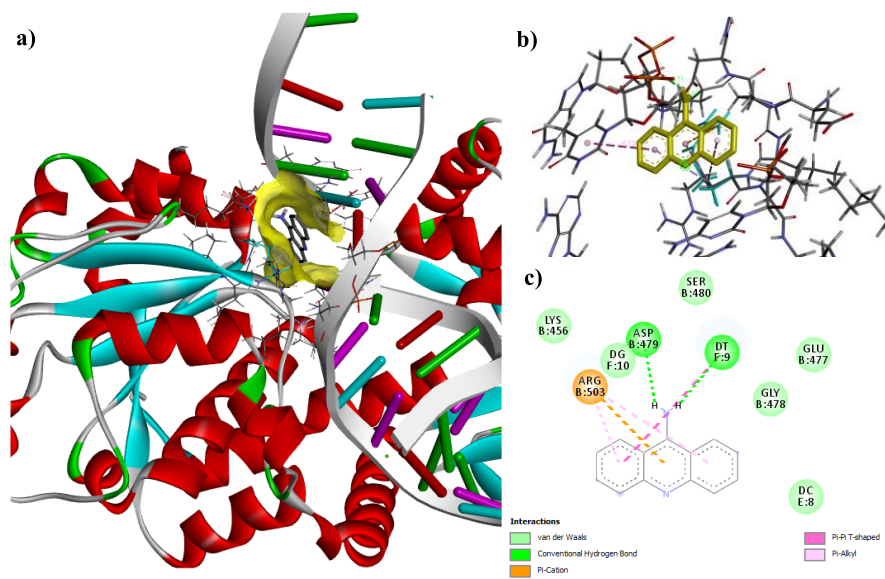


**Figure 9.** The 3D and 2D docking mode of 9-Aminoacridine with topo II $\beta$  (PDB ID:3QX3).

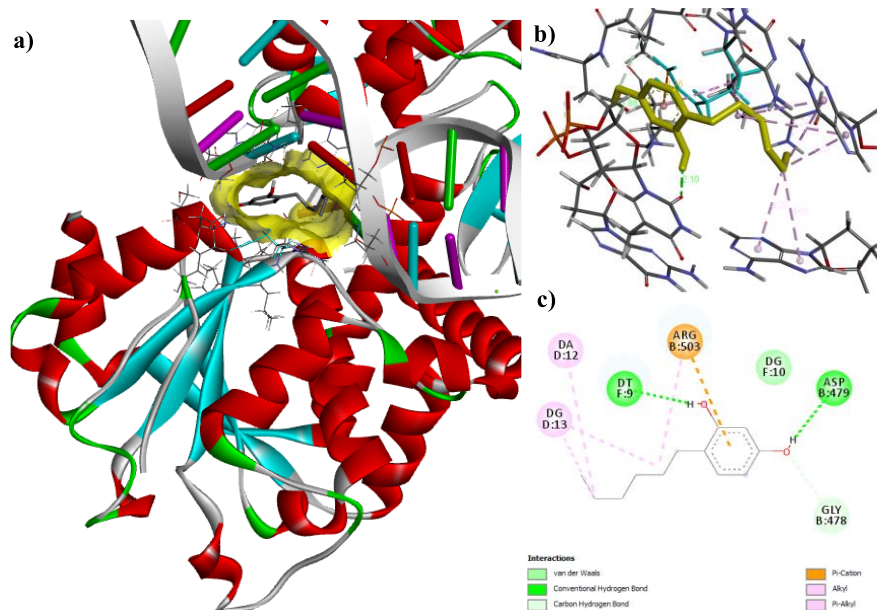


**Figure 10.** The 3D and 2D docking mode of hexylresorcinol with topo IIβ (PDB ID:3QX3).